Chinese Chemical Letters 36 (2025) 110368

Contents lists available at ScienceDirect

Chinese Chemical Letters

journal homepage: www.elsevier.com/locate/cclet

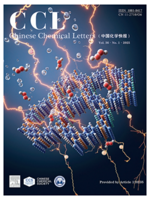

Mini review: Strategies for enhancing stability of high-voltage cathode materials in aqueous zinc-ion batteries

Lingjiang Kou[a,b], Yong Wang[a], Jiajia Song[a,b,*], Taotao Ai[a,*], Wenhu Li[a], Mohammad Yeganeh Ghotbi[c,d], Panya Wattanapaphawong[b], Koji Kajiyoshi[b,*]

[a] *School of Materials Science and Engineering, Shaanxi University of Technology, Hanzhong 723000, China*
[b] *Research Laboratory of Hydrothermal Chemistry, Faculty of Science and Technology, Kochi University, Kochi 780-8081, Japan*
[c] *Institute of Power Engineering (IPE), Universiti Tenaga Nasional, Kajang, Selangor 43000, Malaysia*
[d] *Materials Engineering Department, Faculty of Engineering, Malayer University, Malayer, Iran*

ARTICLE INFO

Article history:
Received 17 June 2024
Revised 10 August 2024
Accepted 24 August 2024
Available online 25 August 2024

Keywords:
Aqueous zinc ion battery
High-voltage cathode materials
Stability enhancement
Failure mechanisms
Electrolyte optimization

ABSTRACT

As battery technology evolves and demand for efficient energy storage solutions, aqueous zinc ion batteries (AZIBs) have garnered significant attention due to their safety and environmental benefits. However, the stability of cathode materials under high-voltage conditions remains a critical challenge in improving its energy density. This review systematically explores the failure mechanisms of high-voltage cathode materials in AZIBs, including hydrogen evolution reaction, phase transformation and dissolution phenomena. To address these challenges, we propose a range of advanced strategies aimed at improving the stability of cathode materials. These strategies include surface coating and doping techniques designed to fortify the surface properties and structure integrity of the cathode materials under high-voltage conditions. Additionally, we emphasize the importance of designing antioxidant electrolytes, with a focus on understanding and optimizing electrolyte decomposition mechanisms. The review also highlights the significance of modifying conductive agents and employing innovative separators to further enhance the stability of AZIBs. By integrating these cutting-edge approaches, this review anticipates substantial advancements in the stability of high-voltage cathode materials, paving the way for the broader application and development of AZIBs in energy storage.

1. Introduction

Secondary batteries, known for their high efficiency and environmental adaptability, are a key focus in energy storage research [1]. As a leading force in energy storage technology, lithium-ion batteries (LIBs) stand out for their versatility and widespread use [2]. LIBs generally use organic electrolytes to realize a wide electrochemical window of >3 V, and thus have a higher energy density than aqueous ion batteries [3,4]. However, organic electrolytes not only carry toxicity and flammability risks but also present serious safety and environmental concerns when mishandled, thus posing significant risks and challenges for large-scale energy storage applications [5]. Table 1 compares the performance characteristics of various common secondary batteries [6-19].

Researchers have been exploring to replace organic electrolytes with aqueous electrolytes [20]. Comparatively, aqueous electrolytes offer environmental friendliness and safety, with ionic conductivity greater than that of organic electrolytes. This feature not only enables high power of battery but also eliminates the need for stringent manufacturing conditions associated with organic electrolytes, leading to significant cost reductions in production [21,22]. Hence, the safety and cost-effectiveness of aqueous ion batteries render them highly promising for large-scale energy storage applications. However, a significant challenge arises from the limitation imposed by the aqueous electrolyte on the operating voltage of battery [23-25]. The cell voltage is ultimately confined by the electrochemical stability window (ESW) of electrolytes. This is because the operating voltage of a designed battery is determined by the potential difference of redox reactions between cathode and anode, which must fall within the ESW of the electrolyte [26,27]. Compared with the organic electrolyte ($\sim$2–5 V), the ESW of aqueous electrolytes is only approximately $\sim$1.23 V [20,28]. Beyond this window, decomposition of water occurs with the evolution of H_2 and O_2, disabling

---

* Corresponding authors.
E-mail addresses: jjsong@snut.edu.cn (J. Song), aitaotao0116@126.com (T. Ai), kajiyosh@kochi-u.ac.jp (K. Kajiyoshi).

https://doi.org/10.1016/j.cclet.2024.110368

Table 1
Comparison of different batteries.

Batteries	Energy density (Wh/kg)	Energy density (Wh/L)	Life (cycles)	Voltage (V)
Ni-Cd	40–70 [6]	–	>3000 [6]	1.2 [6]
Ni-MH	60–120 [7]	330 [8]	>1000 [9]	1.25 [10]
Lead-acid	30–40 [11]	60–75 [11]	500–1000 [12]	2.0 [11]
Li-ion	120–200 [13]	550–600 [14]	400–1200 [14]	3.2–3.85 [15]
Zn-ion	>250 [16]	>500 [16]	>1000 [16]	0.6–1.75 [16]
Na-ion	170–270 [17]	290–380 [17]	>1000 [18]	2.7–3.0 [19]

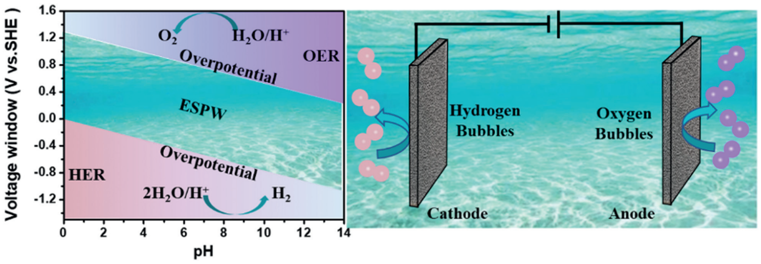

Scheme 1. Pourbaix diagram illustrating the voltage window of aqueous electrolytes, along with a schematic of hydrogen and oxygen production processes.

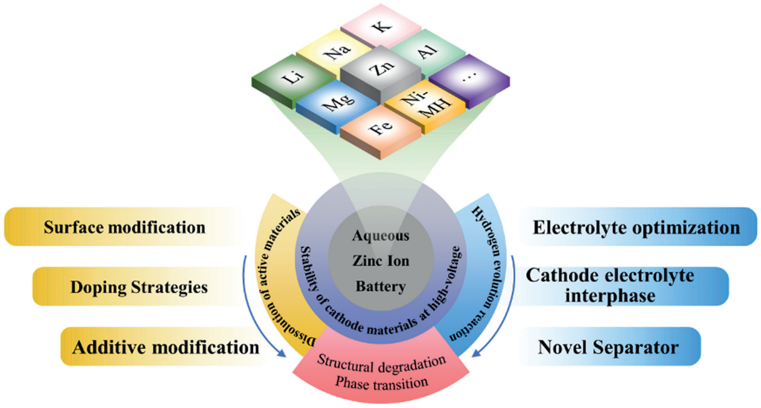

Scheme 2. Overview of failure mechanisms of high-voltage cathode materials in AZIBs and strategies for enhancing cathode stability.

the possibility of redox reaction of electrode materials. The water decomposition process is pH dependent, with the oxygen evolution reaction (OER) and hydrogen evolution reaction (HER) occurring as functions of pH (Scheme 1) [29]. This diagram also illustrates the structural processes involved in the evolution of H_2 and O_2.

AZIBs have emerged as promising candidates for next-generation energy storage systems due to their abundant and low-cost zinc resources, high theoretical capacity, and inherent safety advantages, making them highly prospective for large-scale applications [30,31]. Up to now, reversible Zn^{2+} storage has been investigated in various cathode materials, like manganese oxides (MnO_2 [32], Mn_2O_3 [33], Mn_3O_4 [34], $ZnMn_2O_4$ [35]), vanadium-based materials (VO_2 [36], V_2O_5 [37], $NH_4V_3O_8$ [38], $Na_3V_2(PO_4)_2$ [39], ZnV_2O_4 [40]), Prussian blue analogues (PBAs) ($KCuFe(CN)_6$ [41], ZnHCF [42]), and organic electrode materials (methylene blue [43]). However, these cathodes still face several challenges, including unsatisfactory conductivity, poor reversibility, and limited cycling stability at both high and low temperatures [44-46]. Unlike traditional LIBs, AZIBs utilize water-based electrolytes and earth-abundant materials, making them more sustainable and cost-effective [47]. Despite these advantages, the stability of high-voltage cathode materials remains a critical challenge that hinders their widespread commercialization. Researchers have focused on developing cathode materials with both high operating voltage and capacity [48]. However, the lifespan of these cathodes is often limited due to poor interfacial stability between the cathode and electrolyte. This instability can accelerate cathode degradation increase the risk of electrolyte decomposition, and pose safety hazards such as dendrite formation and internal short circuits. To address these challenges and enhance the interfacial stability, various strategies are being explored and implemented. These strategies include electrolyte formulation optimization, surface modification of cathode materials, incorporation of protective layers or coatings, and advanced interface engineering techniques [49,50]. By improving the interfacial stability, it is anticipated that the lifespan of high-voltage AZIBs can be significantly extended, paving the way for their broader application in energy storage systems.

To date, many research articles and reviews have explored ways to enhance the energy density and operating voltage of AZIBs. However, there is a notable lack of review articles that specifically analyze and summarize the stability of cathode materials under high-voltage conditions. We believe it timely and necessary to present a review on this research to provide recent advances and guidance for enhancing AZIBs performance. The subsequent sections of this review will delve deeper into the basic specific failure mechanisms and then explore promising strategies for improving the stability of high-voltage cathode materials, including surface coating, doping, electrolyte design, conductive additive modification, and separator modifications. Finally, the challenges and perspectives for the stability of high-voltage AZIBs cathode are discussed. Scheme 2 provides a visual summary of the critical issues addressed in the paper and the innovative approaches proposed for enhancing the performance and longevity of AZIBs. By understanding these complexities and advancements, we aim to provide insights and directions for overcoming the existing challenges and accelerating the development of high-performance AZIBs.

2. Failure mechanism of cathode under high-voltage in AZIBs

The stability and behavior of cathode active materials are crucial for understanding the failure mechanisms of AZIBs under high-voltage conditions [51]. As the primary component responsible for energy storage in batteries, the cathode's performance directly impacts the overall battery performance and cycle life. When operated at elevated voltages, these cathode materials are susceptible to various failure mechanisms. The most significant issues often include the dissolution of the cathode active materials, phase transitions, structural damage, and the interactions with the electrolyte. This section will explore these specific failure mechanisms, providing comprehensive insights into the performance degradation and underlying causes of failure observed in AZIBs under high-voltage conditions.

2.1. Dissolution of cathode active materials

Manganese-based materials are considered promising cathode candidates for AZIBs. However, the dissolution of Mn, leading to a rapid capacity drop, along with sluggish electrochemical reaction kinetics, remains a primary obstacle to their further advancement [52]. The loss of Mn in cathode active materials results in structural degradation and capacity attenuation of the electrode. Additionally, Mn deposition at the cathode side, driven by the electric field, affects the cathode electrolyte interphase (CEI) stability, which is critical for cathode's performance.

The detrimental impact of Mn dissolution on the performance of Mn-based materials has prompted researchers to investigate its underlying mechanisms. Currently, electrolyte-induced corrosion is widely recognized as the primary cause of Mn dissolution during cycling. In this process, high-valence Mn cations are susceptible to reduction, transitioning from higher valence states like Mn^{3+} to Mn^{2+}, as part of charge compensation mechanisms involving Mn. Additionally, the Jahn-Teller effect associated with Mn^{3+} contributes to Mn dissolution by promoting the formation of Mn^{2+} through the disproportionation reaction of Mn^{3+} ($Mn^{4+} + e^- \rightarrow Mn^{3+}$; $2Mn^{3+} \rightarrow Mn^{4+} + Mn^{2+}$).

In addition to Mn-based materials, the dissolution of vanadium (V)-based materials is also a significant concern. V-based cathodes, such as V_2O_5 and its derivatives, are attractive due to their high capacity and potential for multi-electron reactions. However, similar to Mn-based materials, V dissolution presents challenges. The dissolution of V cations, particularly V^{5+}, can occur due to electrolyte-induced corrosion and redox reactions. For example, in V_2O_5-based cathodes, V^{5+} can be reduced to V^{4+} or V^{3+} during cycling, leading to structural instability and capacity fading. Studies have shown that the solubility of V^{5+} in the electrolyte can significantly affect the overall performance of V-based cathodes. Efforts to mitigate V dissolution include optimizing the electrolyte composition and incorporating stabilizing agents to enhance the stability of the vanadium oxide framework.

Furthermore, the dissolution behavior of PBAs as a cathode material in AZIBs is a critical factor influencing its performance degradation. PBAs, with the general formula $Fe_4[Fe(CN)_6]_3$, exhibits a complex dissolution mechanism in aqueous electrolytes. The dissolution is primarily driven by the interaction between the electrolyte and the crystal structure of PBAs, where the stability of the $[Fe(CN)_6]^{4-}$ framework is compromised. Studies have shown that the dissolution of iron ions from the PBAs framework is exacerbated by the electrochemical cycling, particularly under conditions where Zn^{2+} diffuse into the lattice. This diffusion not only disrupts the structural integrity but also accelerates the leaching of active iron species. Additionally, the presence of water molecules in the electrolyte can lead to hydrolysis, further contributing to the dissolution of PBAs. Therefore, understanding and mitigating the dissolution mechanism of PBAs in aqueous environments is essential for enhancing the long-term stability and performance of AZIBs.

2.2. Structural degradation or phase transition

The structure integrity of cathode materials is crucial for maintaining the performance and longevity of AZIBs under high-voltage conditions. High voltages can induce various structural changes in cathode materials, significantly affecting their electrochemical properties and overall battery performance [53].

One of the primary structural changes observed in cathode materials under high-voltage conditions is structural degradation. This degradation often involves the deterioration of the crystal structure, leading to reduced active sites for ion intercalation and decreased capacity retention over cycling. The morphology of the cathode material also changes under high-voltage conditions. The degradation can be attributed to the mechanical stress induced by high voltages and the chemical instability of the cathode material in contact with the electrolyte.

To elaborate on these points, the following examples and mechanisms are provided:

(1) Vanadium-based cathodes (*e.g.*, V_2O_5)

V_2O_5 and its derivatives undergo structural water loss and irreversible phase transition when cycled at high voltages. The interlayer water in V_2O_5 provides structural stability and ionic conductivity. Loss of this water during cycling leads to phase transitions from orthorhombic to amorphous phase, degrading electrochemical performance [54]. Additionally, the reduction of V^{5+} to lower valence states (V^{4+}, V^{3+}) can cause lattice distortion and collapse, further contributing to capacity fading.

(2) Manganese-based cathodes (*e.g.*, MnO_2)

Manganese-based materials, such as MnO_2, suffer from structural degradation primarily due to the Jahn-Teller effect and Mn dissolution. High-voltage cycling induces the disproportionation reaction of Mn^{3+} ($2Mn^{3+} \rightarrow Mn^{4+} + Mn^{2+}$), leading to the dissolution of Mn^{2+} into the electrolyte. This dissolution not only reduces the amount of active material but also causes structural collapse and capacity loss. The formation of various polymorphs of MnO_2 during cycling can also lead to phase transitions, further impacting the stability and performance of the cathode [55].

(3) PBAs (*e.g.*, ZnHCF)

PBAs, such as zinc hexacyanoferrate (ZnHCF), exhibit high capacity and stability in AZIBs. However, structural degradation can occur due to the loss of crystallinity and framework collapse under high-voltage cycling. The insertion and extraction of Zn^{2+} can induce stress within the crystal lattice, leading to fractures and defects. Additionally, the decomposition of the cyano-bridged network in PBAs can result in the loss of electroactive sites and diminished capacity retention [56].

Furthermore, phase transition phenomena in cathode materials subjected to high voltages involve changes in the atomic arrangement or crystal structure of the material. These transitions can result in altered electrochemical properties, such as capacity, voltage, and cycling stability. High voltages can drive these phase transitions by providing the necessary energy to overcome the activation barriers between different phases or structural states.

2.3. Hydrogen evolution reactions

While aqueous electrolytes offer inherent safety and cost-effectiveness, the anode electrode Zn faces thermodynamic instability in this environment. Even during the battery standby, hydrogen precipitation occurs at the interface between the aqueous electrolyte and the cathode [57]. On the cathode side, the process of HER occurs:

$$H_2O + 2e^- \rightarrow H_2 + 2OH^- \text{ (neutral/alkaline)} \tag{1}$$

$$2H^+ + 2e^- \rightarrow H_2 \text{ (acidic)} \tag{2}$$

The HER occurring at the cathode-electrolyte interface play a critical role in the degradation of AZIBs. The reaction involves complex electrochemical processes to form H_2. The generation of H_2 not only leads to the loss of active cathode and electrolyte but also affects the overall performance and safety of the battery. The electrochemical processes involved in HER and their implications for battery performance are essential considerations in understanding and addressing the challenges posed by thermodynamic instability in AZIBs. This overlooked concern significantly impacts the calendar life of the battery, a parameter as crucial as the extensively studied cycle life.

3. Improving stability of cathode materials under high-voltage

3.1. Surface modification and doping strategies

Surface modification provides a controllable method to stabilize the electrode/electrolyte interface and reduce the side reactions, especially under high-voltage conditions. Additionally, the incorporation cations and anions has been considered an effective way to improve the electronic and ionic conductivity of cathode materials.

3.1.1. Surface modification

Coating a protective layer on the surface of cathode materials is considered an attractive strategy to improve interfacial stability, particularly because parasitic reaction predominantly occurs at the interface cathodes and electrolytes. Under high-voltage conditions, increased voltage stress on the cathode material may induce parasitic reactions at the CEI layer, leading to the formation of unstable deposits and degradation of the cathode material, thus impacting its stability. Various kinds of coating layers have been introduced to act as an artificial CEI, such as inorganic phase and organic species can be served as coating materials. For the use of inorganic materials as cladding materials, the common inorganic materials are MgO [58], Al_2O_3 [59], and TiO_2 [60]. For the organic species coating, polymer materials (polyacrylonitrile (PAN), 3,4-ethylenedioxythiophene (PEDOT), polypyrrole (PPy)) were used to improve the electronic conductivity of cathode materials.

For example, the carbon coating layer on $NaVPO_4F$ (C–$NaVPO_4F$) to form a stable surface layer, improving its electronic conductivity and stability [61]. The C–$NaVPO_4F$ was prepared by a facile soft template method. SEM analysis reveals that C–$NaVPO_4F$ is composed of irregular primary particles, exhibiting diameters spanning from 100 nm to 200 nm (Fig. 1a). In Fig. 1b, it is evident that the $NaVPO_4F$ particles are enveloped by a uniform, transparent carbon coating measuring 20 nm in thickness. In Fig. 1c, the Raman spectrum provides insights into the structural characteristics of the material, with the intensity ratio (I_D/I_G) of the diffraction peaks indicating the degree of graphitization and defect density within the carbon coating. For the C–$NaVPO_4F$ sample, the calculated I_D/I_G value of 0.94 signifies a notable degree of graphitization, implying a well-ordered and crystalline nature of the carbon cladding layer, suggesting enhanced electrical conductivity and stability. When the battery was operated in a voltage rage of 0.6–1.8 V at 0.05 A/g, a voltage plateau of 1.36 V was utilized (Fig. 1d). Additionally, the long-term cycling performance of the system was assessed at 1 A/g (Fig. 1e). Remarkably, even after the 4000^{th} cycles, the battery exhibited superior capacity retention is 89.3%. The outstanding cycling stability observed in this study can be attributed to the synergistic effects of the electrolyte and the carbon coating layer, which collectively enhance the stability of $NaVPO_4F$, particularly at high operating voltages.

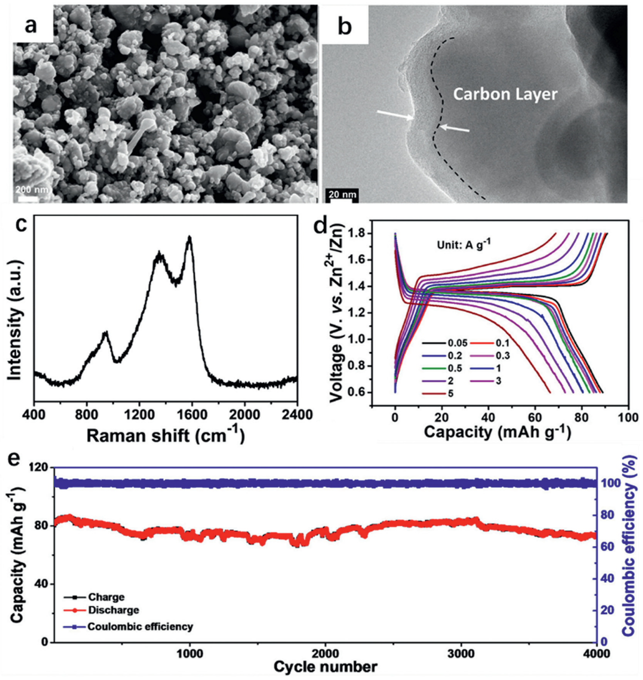

Fig. 1. Morphology and performance of carbon-coated $NaVPO_4F$ sample: (a, b) SEM and TEM; (c) Raman spectrum; (d) Galvanostatic charge-discharge curves at various current density from 0.05 A/g to 5 A/g; (e) Long-term stability of the battery at 1 A/g. Adapted with permission [61]. Copyright 2021, American Chemical Society.

In addition to carbon layer coating technology, coating with polymer materials is also an important method to enhance the stability of cathode materials. Such as PAN, PEDOT, and PPy, exhibit significant advantages in improving electrode performance due to their excellent conductivity and flexible chemical structures. The research by Saiful Islam *et al.* [62] on the $Na_{1.1}V_3O_{7.9}$ (NVO) nanorod cathode coated with PPy (P-NVO) provides significant insights into enhancing the stability of cathode materials for AZIBs, particularly under high-voltage conditions. The study demonstrates that PPy coating not only improves the electronic conductivity and Zn^{2+} diffusion kinetics but also significantly stabilizes the NVO structure at elevated voltages, thereby ensuring the effective utilization of the $V^{3+}/V^{4+}/V^{5+}$ redox reactions in the NVO cathode. This leads to a higher discharge capacity, improved power capability, and superior cycling stability compared to the uncoated NVO cathode. Fig. 2a is the schematic illustration of the structure of P-NVO. From Figs. 2b and c, it can be found that the morphology of P-NVO is a rough surface nanorod, and further high-resolution TEM (Fig. 2d) reveals a uniform PPy layer with a thickness of 9 nm on the surface of NVO. The TGA curves also confirm that the PPy coating layer on the surface of NVO (Fig. 2e). Notably, even at a high current density of 6000 mA/g, the P-NVO cathode exhibits outstanding cycling stability over 1100 cycles without capacity loss (Fig. 2f). This significant enhancement in performance, particularly at high voltages, is attributed to the conductive PPy layer, which

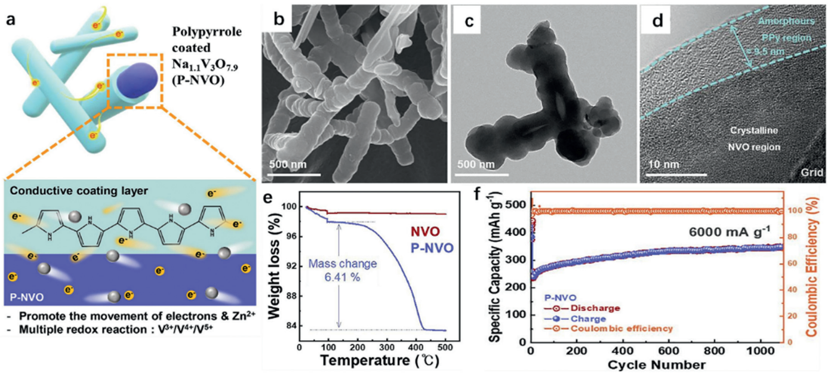

Fig. 2. (a) Schematic illustration of the P-NVO cathode for AZIBs; (b) SEM, (c, d) TEM images of P-NVO; (e) TGA curves comparing NVO and P-NVO; (f) Cycling performance of P-NVO at a current density of 6000 mA/g. Adapted with permission [62]. Copyright 2022, Elsevier.

acts as a protective shield, enhancing the structural integrity and electronic properties of the NVO nanorods under demanding electrochemical conditions.

Similarly, Liu *et al.* [63] propose a medication strategy using a polyaniline (PANI) coating on ZnHCF. The PANI coating inhibits the dissolution of ZnHCF and enables the AZIBs to present two long-flat discharge voltage platform as well as a high capacity of 150 mAh/g, which provides a new idea for the development of high-performance PBAs battery material.

These examples illustrate the effectiveness of surface modification strategies in improving the stability and performance of cathode materials in AZIBs. By combining surface coatings with other approaches such as electrolyte optimization and conductive additive innovations, we can achieve synergistic effects that further enhance battery performance and longevity.

3.1.2. Doping strategies

Building upon the foundation of surface modification, we now turn our attention to doping strategies. Doping involves the intentional introduction of foreign atoms into the crystal lattice of cathode materials to modify their electronic and ionic properties, and improve the interface stability [64]. In AZIBs cathode materials, doping elements are generally divided into two categories: metallic elements (such as Ca, Ni, Ti, Fe, and Na) and non-metallic elements (such as N and S).

For instance, doping S into MnO_2 can enhance the intrinsic electronic conductivity and accelerate the reaction kinetics [32]. Similarly, the introduced of Na^+ into the interlayer of V_2O_5 not only improves structure robustness but also enhances electronic conductivity by stabilizing the $[V_4O_{12}]_n$ layers [65].

A recent study by Wu *et al.* [66] demonstrates the effectiveness of Fe-doping in enhancing the performance of vanadium oxide (VO) for AZIBs. Their work shows that Fe-doped vanadium oxide (FeVO) nanobelts exhibit significantly improved structural stability and electrochemical performance under high-voltage conditions. The schematic illustration of the preparation process and the crystal model of FeVO, as shown in Fig. 3a, highlights the introduction of Fe into the vanadium oxide lattice. The XRD patterns in Fig. 3b confirm the successful doping of Fe into the V_2O_5 structure, with FeVO showing a characteristic peak at 8.17°, corresponding to the (001) crystal plane with a lattice spacing of 10.8 Å, indicative of expanded interlayer spacing which facilitates Zn^{2+} diffusion. The SEM image in Fig. 3c depict the nanobelt morphology of FeVO, while the HRTEM and STEM-EDX elemental mapping in Figs. 3d and e, respectively, illustrate the uniform distribution of Fe within the nanobelt structure. The cycling performance (Fig. 3f) reveals that FeVO maintains a high capacity retention of 94.6% after 300 cycles at 0.5 A/g, outperforming undoped VO and commercial V_2O_5. This enhanced performance is attributed to the stabilized layered structure and the rapid Zn^{2+} diffusion channel created by Fe-doping, which mitigates the structure degradation commonly observed in vanadium-based cathodes during cycling.

To illustrate the beneficial of non-metal atom doping on the electrochemical performance and structure stability of cathode materials in AZIBs, the work by Cui *et al.* [67] on N doped KMn_8O_{16} (N-KMO) serves as a compelling example. The introduction of N doping and oxygen vacancies significantly improved the electrical conductivity and structural stability of KMn_8O_{16}. The synthesis process and N doped crystal structure are depicted schematically in Fig. 4a. Elemental mapping *via* STEM-EDX (Fig. 4b) confirms the uniform distribution of N within the N-KMO structure. Figs. 4c and d illustrate the improved electrochemical performance under high-voltage plateaus (~1.4 V). Notably, Fig. 4e displays the mass content of dissolved Mn in aqueous electrolyte during cycling, highlighting N doping can effectively inhibit the dissolution of Mn. Finally, as shown in Fig. 4f, N-KMO demonstrate a high reversible capacity of 262 mAh/g after 2500 cycles at a current density of 1 A/g, maintaining 91% of initial capacity. These results clearly demonstrate that N doping, in combination with oxygen vacancies, effectively enhances the structural stability and electrochemical performance of cathode materials in AZIBs. Zhang *et al.* [68] prepared a N-doped ε-MnO_2 (MnO_2@N) using electrochemical deposition and heat treatment under nitrogen atmosphere. As the cathode for ZAIBs, the capacity retention rate of MnO_2@N cathode is close to 100% after 500 cycles at 0.5 A/g. And it can be found that the oxygen vacancies increase after nitrogen doping, which can improve the conductivity of the MnO_2@N cathode. Also, there is Mn-N bond in MnO_2@N, which can enhance the electrochemical stability of MnO_2@N cathode.

3.2. Electrolyte optimization

The stability and performance of cathode materials in high-voltage applications are not determined by their intrinsic properties but also significantly influenced by the electrochemical environment, particularly the electrolyte. Optimizing the electrolyte composition and the CEI is essential for mitigating side reactions, improving Zn^{2+} conductivity, and preserving structural integrity during cycling. The electrolyte plays a critical role in the overall electrochemical behavior of the battery, affecting the formation of CEI, the dissolution of cathode materials, and ultimately the battery's lifespan.

3.2.1. Cathode electrolyte interfacial electrochemical behaviors

The electrochemical behavior of the CEI in AZIBs is complex due to the high reactivity of the aqueous electrolyte and its limited

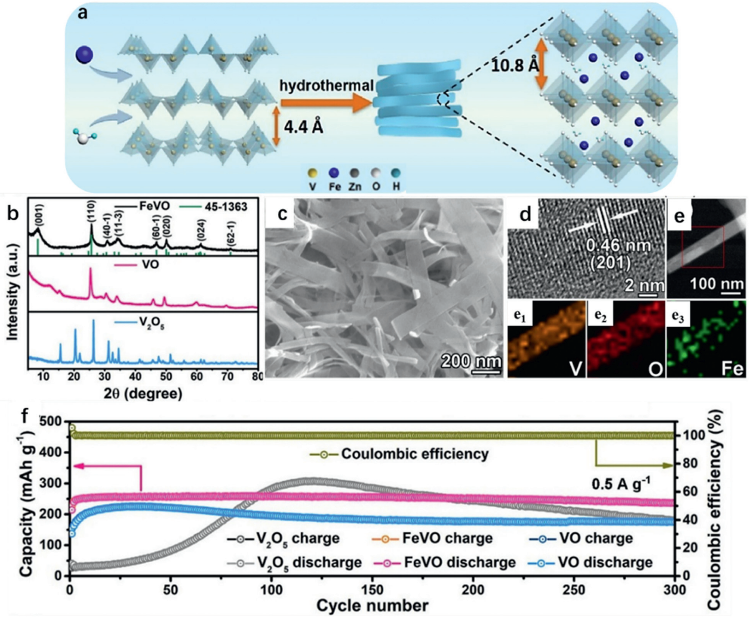

Fig. 3. (a) Schematic illustration of the preparation and the crystal model of FeVO. (b) XRD patterns of FeVO, VO and commercial V_2O_5. (c) SEM images; (d, e) HRTEM and STEM-EDX elemental mapping of FeVO nanobelt. (f) Cycling performance of FeVO, VO and commercial V_2O_5; at 0.5 A/g. Adapted with permission [66]. Copyright 2021, Elsevier.

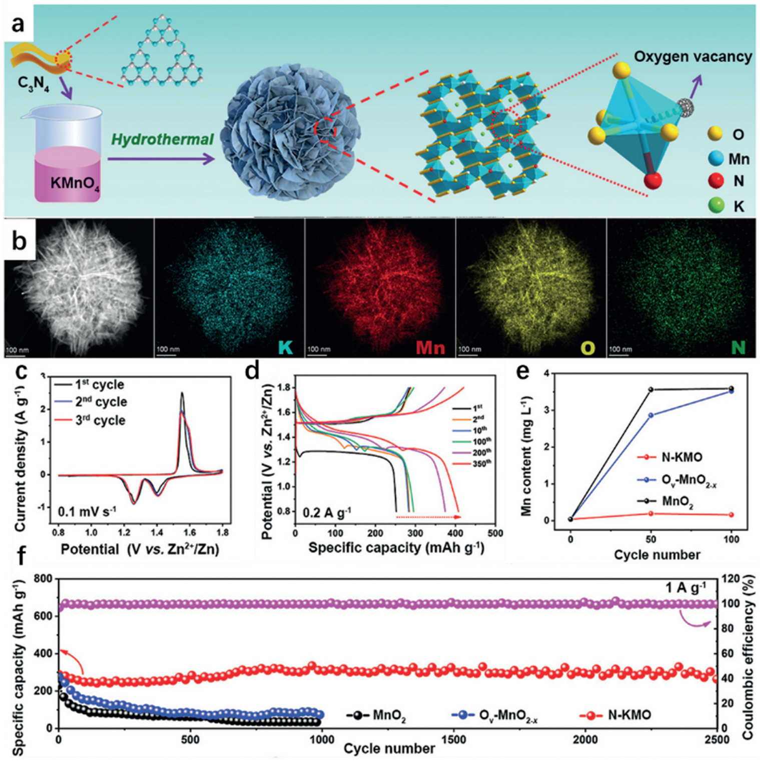

Fig. 4. (a) Schematic illustration of the synthesis and the N doped crystal structure. (b) STEM-EDX elemental mapping, (c) CV curves at a scan rate of 0.1 mV/s. (d) GCD curves at a current density of 0.2 A/g of N-KMO. (e) Mass content of dissolved Mn in a 2 mol/L $ZnSO_4$ aqueous electrolyte during cycling. (f) Cycling performance at a current density of 1 A/g of MnO_2, O_v-Mn_{2-x}, and N-KMO. Adapted with permission [67]. Copyright 2022, Wiley-VCH.

ESW. At the CEI, both zinc storage and HER can occur, which constrain the battery's output voltage. The CEI's behavior during cycling plays a crucial role in determining the electrochemical properties of the cathode materials. During Zn^{2+} storage, the transport of Zn^{2+} involves three key steps: (1) De-solvation of Zn^{2+} from their dissolved state on the cathode surface, (2) migration of Zn^{2+} through the interfacial reaction products, and (3) solid-state diffusion within the bulk cathode material [69]. Among these, the desolvation process at the CEI is the rate-determining step and is crucial to the overall electrochemical reaction.

The formation of the CEI results from the interaction between oxide-based cathode materials (*e.g.*, MnO_2 and V_2O_5) and H^+ during cycling. Side reaction involving OH^- with electrolyte salts, such as $ZnSO_4$ (Fig. 5a), lead to the depletion of H^+ and the formation

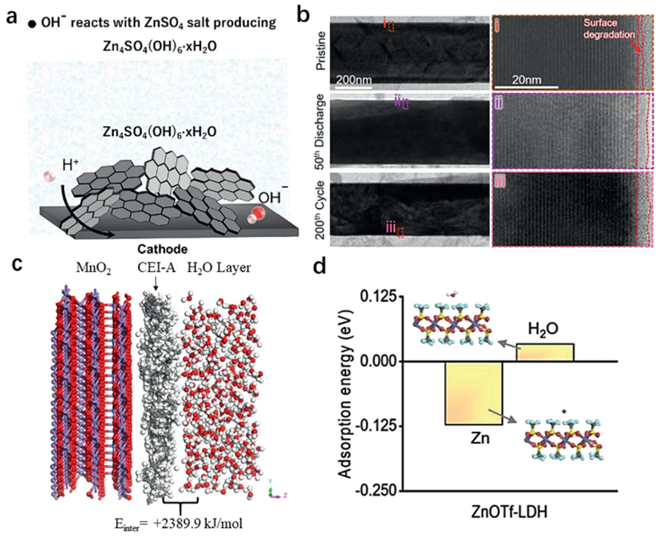

Fig. 5. (a) Schematic illustration of the formation and composition of CEI. Adapted with permission [70]. Copyright 2022, Chinese Academy of Sciences. (b) TEM images of cycled states of the V-based oxide cathode surface. Adapted with permission [71]. Copyright 2022, American Chemical Society. (c) Theoretical calculation of interaction energy (E_{inter}) from alkane/H_2O interfaces. Adapted with permission [72]. Copyright 2022, American Chemical Society. (d) Adsorption energy of Zn^{2+} and H_2O in the channel of ZnOTf-LDH. Adapted with permission [73]. Copyright 2024, Wiley-VCH.

of a loose and porous CEI layer [70]. This layer can develop cracks upon contact with the electrolyte, allowing the aqueous electrolyte to penetrate and reach the interior of the cathode. When the aqueous electrolyte contacts the cathode, H^+ and OH^- ions can react with the cathode material (*e.g.*, V-based oxides), cousing lattice degradation (Fig. 5b) [71]. Liu *et al.* [72] have effectively demonstrated the interaction energy at the alkane-H_2O interface (CEI-A) through theoretical calculations (Fig. 5c). The artificially prepared CEI-A can effectively reduce both Mn dissolution and the contact of conductive graphite with water. This inhibition prevents the reaction: $C + xH_2O \rightarrow CO_x + 2xH^+ + 2xe^-$, thereby enhancing the stability of the system. Dai *et al.* [73] examined the CEI of $Zn_x(OTf)_y(OH)_{2x-y} \cdot nH_2O$ (ZnOTf-LDH) for its species permeability. DFT calculations revealed that this CEI exhibits hydrophobicity and high affinity for Zn (Fig. 5d), which contribute to stabilizing the interfacial structure and preventing H_2O intercalation.

3.2.2. Interfacial optimization strategies on cathode

Despite extensive research on $ZnSO_4$ and $Zn(OTf)_2$-based electrolytes over the past decades, and ideal electrolyte compatible with high-voltage cathodes has yet to be developed. To achieve reliable CEI with excellent electrochemical properties, mechanical stability, and high ion diffusion coefficient, optimizing electrolytes is considered a highly effective approach. Li *et al.* [74] introduced an environmentally isosorbide dimethyl ether (IDE), as an extruding agent in the aqueous electrolyte. The IDE molecule significantly suppressed the reactivity of water within the electrolyte, promoted the homogeneous nucleation of Zn, and guided its directional growth along the (002) planes. Additionally, IDE contributed to the structural stability of electrode materials. Recent research has demonstrated that the use of an ultralow-water-activity (UWA) electrolyte can significantly improve the stability of vanadium-based cathodes, addressing the issues of vanadium dissolution and structural degradation. In a study by Wang *et al.* [75], the authors introduced a novel UWA electrolyte that incorporates trimethyl phosphate (TMP) as an inert diluent. This design uniquely reduces the free water activity, thereby minimizing parasitic reactions and vanadium dissolution. The UWA electrolyte ensures that most water molecules are solvated with highly concentrated $ZnCl_2$ clusters, leaving only 2.5% of solvation water to coordinate with each other. This configuration significantly inhibits water decomposition and vanadium dissolution, fostering the formation of a robust and stable CEI on the V_6O_{13} cathode. Fig. 6a illustrates the anodic ESW of the $ZnCl_2$ and UWA electrolyte. The oxygen evolution potential of UWA electrolyte is approaching to 1.5 V, demonstrating that the stability of water molecules was increased. And the structure degradation caused by vanadium dissolution and water decomposition was extremely decreased. Dissolution of vanadium was also researched by elemental content analysis (Fig. 6b). As depicted in Fig. 6c, the degradation mechanism involves interactions with H^+ and OH^-, which are effectively suppressed by the UWA electrolyte, leading to enhanced cathode and CEI stability. The formation of a stable CEI layer is critical for preventing vanadium dissolution and enhancing the overall stability of the cathode (Figs. 6d and e). As shown in Fig. 6f, the V_6O_{13} cathode demonstrates remarkable capacity retention of 99.43% after 3000 cycles at a current density of 1 A/g. These enhancement are attributed to the stable CEI formed in the UWA electrolyte, which effectively prevents vanadium dissolution and water shuttling between the cathode and the electrolyte.

At the same time, introducing appropriate metal cations into the electrolyte can mitigate the dissolution of the cathode material and prolong the cycle life, especially for Mn-based materials that are susceptible to neutral and weakly acidic electrolytes. For example, Zhang *et al.* [76] found that adding $Mn(CF_3SO_3)_2$ significantly alleviated the irreversible dissolution of Mn^{2+} caused by the Jahn-Teller effect. By adding 0.1 mol/L $Mn(CF_3SO_3)_2$ to a 3 mol/L $Zn(CF_3SO_3)_2$ electrolyte, the introduced Mn^{2+} produced uniform porous MnO_x nanosheets on the surface of β-MnO_2, which inhibited the dissolution of β-MnO_2.

3.3. Innovations in conductive additive modification

Introducing conductive additives into electrodes effectively enhances electronic conductivity, reduces polarization during high current density cycles, improves electrolytes adsorption, and lowers internal resistance. These improvements significantly boost the overall rate performance of AZIBs. Despite their small proportion by mass, conductive additives play a crucial role in determining the power and energy density of AZIBs. One of the notable study in this area by Huang *et al.* [77] highlights the effectiveness of a binary conductive additive comprising carbon nanohorns (CNHs) and carbon nanotubes (CNTs) for the MnO_2 cathode in AZIBs. As depicted in Figs. 7a-c, the CNTs/CNHs network establishes high-speed electron channels, with CNTs providing a conducting pathway and CNHs offering additional surface area for electron transfer. The SEM image in Fig. 7d shows MnO_2 embedded in a conducting network of CNTs and CNHs, where CNHs aggregates fill the gaps between CNTs and MnO_2, facilitation closer physical contacts and improving electron transport. Fig. 7e shows the discharge plateau for MnO_2–CNTs/CNHs was higher at 1.36 V, which demonstrates stable voltage profiles and high capacity retention. The MnO_2 cathode with CNTs/CNHs additive achieves a specific capacity of 191.3 mAh/g at 3 A/g, and maintains 96.5% of its initial capacity after 500 cycles (Fig. 7f). This binary additive strategy offers new pathways for optimizing the design and functionality of advanced AZIBs cathodes, making it a promising technique for future energy storage applications.

3.4. Novel separator materials

The separator is a crucial component in secondary batteries, acting as an insulating barrier between the cathode and anode. Its primary function is to prevent direct electron flow between the

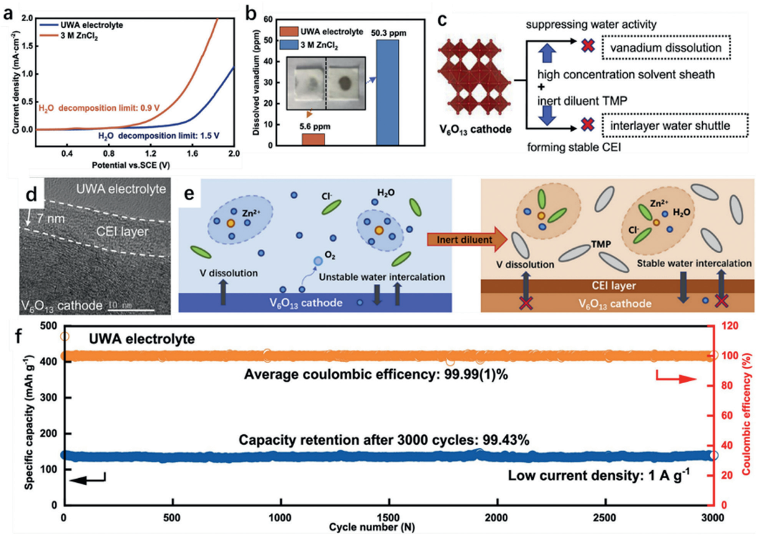

Fig. 6. (a) Anodic ESW. (b) Elemental analysis of dissolved vanadium ions in the electrolyte after the 1st cycle (inset: photos of the separator). (c) Proposed degradation mechanism of the V_6O_{13} cathode and the effects of UWA electrolyte on cathode stability. (d) CEI structure on V_6O_{13} cathode interphase in UWA electrolyte after 10 cycles. (e) Schematic of vanadium dissolution and CEI formation in UWA electrolyte. (f) Cycling performance at 1 A/g. Adapted with permission [75]. Copyright 2022, Elsevier.

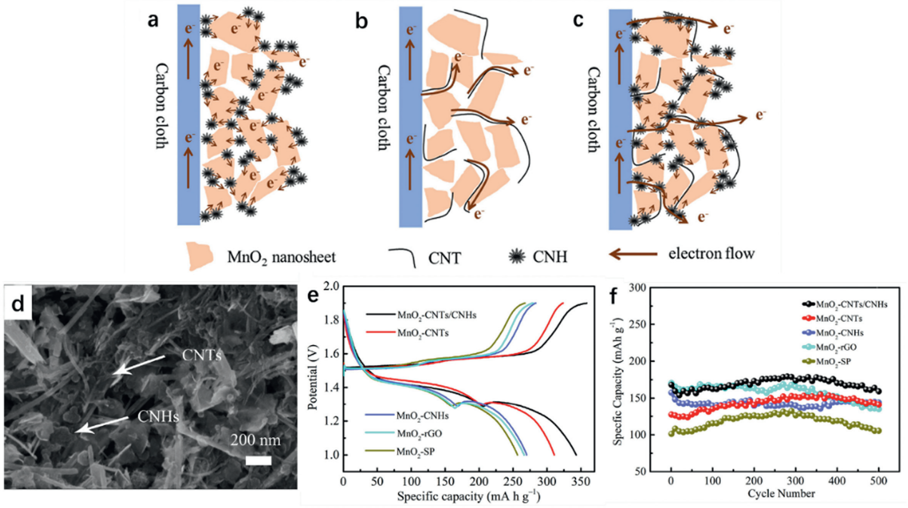

Fig. 7. (a-c) Schematics of electron pathway in MnO_2−CNHs, MnO_2−CNTs, and MnO_2−CNTs/CNHs electrode. (d) SEM image of MnO_2−CNTs/CNHs. (e) Galvanostatic charge and discharge profiles of the 4th cycle at 0.3 A/g. (f) Cycling performance at 3 A/g of MnO_2−CNTs/CNHs, MnO_2−CNTs, MnO_2−CNHs, MnO_2-rGO and MnO_2-SP electrodes. Adaped with permission [77]. Copyright 2020, Elsevier.

electrodes while allowing ion transport through its porous structure, ensuring the battery operates both efficiently and safely. Additionally, the separator stores the electrolyte needed to create ion migration channels during electrochemical reactions. Glass fibers (GF), filter paper, and hydrophilic polyolefins are commonly used as separators in ZIBs, with GF being the most widely utilized. Although GF separators are highly porous and extremely hydrophilic, they suffer from low mechanical strength, which makes them incapable of withstanding the formation of zinc dendrites. Additionally, the considerable thickness of GF separators (600 μm) occupies excessive space within the cell and contributes to high costs, making it challenging to control the cost per unit of cell energy density. If the separator fails to mitigate the dissolution of the cathode material, the performance of the cathode will be significantly compromised due to the loss of active material. Consequently, various strategies have been employed to functionalize the separator to enhance their performance and effectiveness in AZIBs [78].

Metal-organic framwork (MOF) are porous crystalline material that self-assemble from metal ions and organic ligands. They possess an extensive pore volume, high specific surface area, and adjustable pore sizes, facilitating uniform ion transport. Due to Zr-based MOF exceptional chemical and thermal stability, mechanical robustness and high surface area with tunable porosity. These properties make them for maintaining structure integrity and performance in the demanding conditions of AZIBs, ensuring efficient Zn^{2+} transport and enhanced battery safety. A recent study by Song *et al.* [79] investigates the use of a Zr-based metal-organic framework (MOF) functionalized GF separator, known as (UiO-66-GF), to enhance the electrochemical performance of AZIBs. The UiO-66-GF separator improves charge carrier transport and favors the orientation of the (002) crystal plane, which enhances corrosion resistance and enables dendrite-free zinc deposition. To evaluate the efficacy of the UiO-66-GF separator, full cell with an α-MnO_2 cathode were assembled (Zn|UiO-66-GF|MnO_2). Fig. 8a presents a schematic diagram of the full cell model. The presence of Ui-66 promotes the preferential orientation of the (002) crystal plane, promoting the horizontal growth of Zn^{2+} and effectively preventing dendrites formation (Figs. 8b and c). DFT calculations

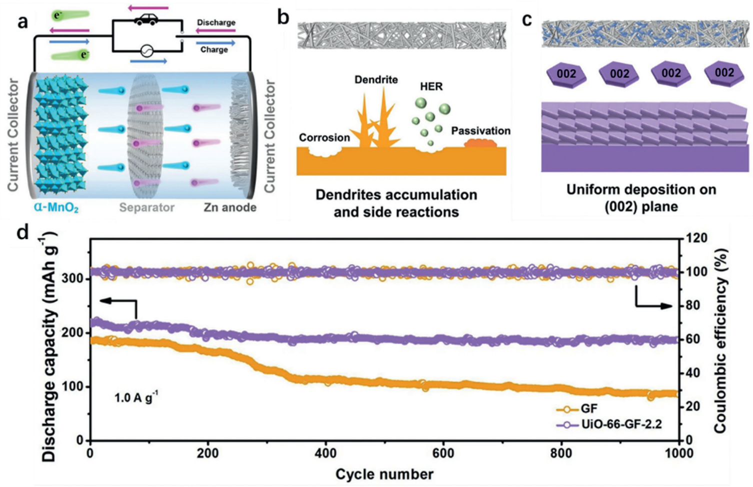

Fig. 8. (a) Electrochemical behavior of Zn|UiO-66-GF|MnO_2 cell. (b, c) Mechanism comparison of the deposition process for zinc anodes using GF and UiO-66-GF-2.2. (d) Cycle performance of Zn|GF|MnO_2 and Zn|UiO-66-GF-2.2|MnO_2 at 1.0 A/g. Adapted with permission [79]. Copyright 2022, the Authors.

indicate that the (002) crystal surface exhibits weakened adsorption of H, which enhances the corrosion resistance of the Zn anode and effectively suppresses the hydrogen evolution reaction (HER). As shown in Fig. 8d, the full cell (Zn|UiO-66-GF-2.2|MnO_2) demonstrates excellent long-term cycling stability, maintaining a high discharge capacity of 186.55 mAh/g after 1000 cycles with a capacity retention of 85%. This study highlights the significant role of advanced separator materials in enhancing battery performance. The innovative approach of using MOF-functionalized separators not only mitigates common issues such as dendrite formation and corrosion but also significantly boosts the cycling stability and capacity retention of AZIBs.

In addition to the use of MOF-functionalized separators, which enhance ion transport and stability in AZIBs, another promising approach involves the development of environmentally friendly biomass nanofibers. For example, Zhang *et al.* [80] constructed such a membrane to replace traditional glass fiber diaphragms in AZIBs. This robust biomass membrane reduces the diaphragm thickness to just 9 µm, effectively preventing Zn dendrite penetration, controlling crystal orientation during Zn deposition, and improving the corrosion resistance of Zn. Consequently, this innovative design not only offers excellent electrochemical performance but also demonstrates a versatile approach to enhancing the performance of metallic Zn anodes through the use of advanced separator materials, rather than modifications to the Zn itself.

In addition to the MOF-functionalized and biomass-based separators, there are other promising approaches to modify separators in AZIBs. Thanks to the robust interaction between cation-attracting organic functional groups and Zn^{2+}, organic-based functionalized separators are essential for managing the Zn^{2+} flow. Cation-selective separators stand out as a key category among these. The common understanding is that the surface of a cation-selective separator is densely populated with active charged groups, which create a double electric layer with oppositely charged ions in the electrolyte. This electric field serves to repel anions while enhancing the absorption and migration of cations. Another key approach to the functional modification of separators is the development of inorganic compound-functionalized separators [78]. These inorganic materials are available in various forms, are easy to prepare, and offer excellent thermal and mechanical stability. Their distinctive properties are highly effective in preventing zinc dendrite penetration, enhancing separator wettability, and regulating ion transport.

4. Conclusion and perspectives

In this review, we have thoroughly explored the challenges and advanced strategies for improving the stability of high-voltage cathode materials in AZIBs. Key failure mechanisms, such as the dissolution of cathode active materials, structural degradation, phase transitions, and HER, have been identified as significant barriers to the performance and longevity of AZIBs. Addressing these challenges is crucial for the development of reliable and efficient high-voltage cathode materials in AZIBs.

4.1. Surface modification and doping strategies

Surface modification and doping have been shown to be effective methods to enhance the stability of cathode materials. Surface modifications, such as coating and creating protective layers, help in mitigating the direct interaction between the cathode and the electrolyte, thus reducing dissolution and structural degradation. Doping strategies further enhance the electrochemical performance by stabilizing the crystal structure and improving ion conductivity.

4.2. Electrolyte optimization

Optimizing the electrolyte composition is essential for stabilizing the CEI. Aqueous electrolytes with tailored compositions can extend the ESW and minimize parasitic reactions. The interfacial electrochemical behaviors at the CEI are critical, with strategies focusing on enhancing Zn^{2+} transport and reducing side reactions. Functionalized electrolytes can significantly improve the cycling performance and stability of the cathode.

4.3. Innovations in conductive additive modification

Incorporating conductive additives into the electrodes enhances electronic conductivity and reduces polarization during high current-density operations. This leads to improved rate performance and overall cell efficiency. Although used in small quantities, conductive additives play a significant role in determining the power and energy density of AZIBs. Advanced conductive additives stabilize the cathode structure and improve electrochemical performance.

4.4. Novel separator materials

Innovative separator materials, such as MOF-functionalized separators, offer promising solutions for stabilizing both anodes and cathodes. These separators enhance charge carrier transport and prevent dendrite formation, significantly improving the cycling stability and capacity retention. The use of MOF-functionalized separators in AZIBs represents a cutting-edge approach to achieving long-term stability and high performance.

4.5. Future perspectives

Future research should focus on further optimizing these strategies and exploring synergistic effects between different approaches. Continued advancements in material science, electrochemistry, and battery engineering are essential for developing next-generation AZIBs with enhanced stability and performance. Emphasis should be placed on scalable and cost-effective solutions to facilitate the commercial adoption of high-voltage AZIBs.

To achieve these goals, several key areas should be addressed: (1) Integration of surface modification and electrolyte optimization. Combining advanced surface modification techniques with optimized electrolytes can create a more stable CEI. For instance, surface coatings that protect against dissolution can work synergistically with electrolytes designed to minimize parasitic reaction, resulting in a significant enhancement in both stability and performance. (2) Synergistic use of conductive additives separator materials. The integration of advanced conductive additives with innovative separator materials can ensure uniform electron and Zn^{2+} transport throughout the cell. Conductive additives improve electronic conductivity, while MOF-functionalized separators enhance Zn^{2+} transport and prevent dendrite formation. (3) Advanced material engineering. Engineering cathode materials to withstand high-voltage cycling is crucial. For example, designing V_2O_5 with interlayer water for structural stability, or MnO_2 with controlled phase transitions, can reduce structural degradation. When these engineered materials are combined with surface modifications, optimized electrolytes, and conductive additives, the overall system performance can be significantly improved.

In conclusion, integration advanced surface modification techniques, optimizing electrolyte, innovating conductive additive, and developing novel separator materials provides a comprehensive strategy to address the challenges of high-voltage cathode materials in AZIBs. These methods not only stabilize the cathode structure but also enhance the overall electrochemical performance, paving the way for the development of robust and efficient energy storage systems for future applications.

Declaration of competing interest

The authors declare that they have no known competing financial interests or personal relationships that could have appeared to influence the work reported in this paper.

CRediT authorship contribution statement

Lingjiang Kou: Writing – review & editing, Writing – original draft, Supervision. **Yong Wang:** Conceptualization. **Jiajia Song:** Writing – review & editing, Writing – original draft. **Taotao Ai:** Funding acquisition. **Wenhu Li:** Funding acquisition. **Mohammad Yeganeh Ghotbi:** Methodology. **Panya Wattanapaphawong:** Resources. **Koji Kajiyoshi:** Resources.

Acknowledgments

This work was supported by the Exchange Program of High-end Foreign Experts of Ministry of Science and Technology of People's Republic of China (No. G2023041003L), the Natural Science Foundation of Shaanxi Provincial Department of Education (No. 23JK0367), and the Scientific Research Startup Program for Introduced Talents of Shaanxi University of Technology (Nos. SLGRCQD2208, SLGRCQD2306, SLGRCQD2133), Contaminated Soil Remediation and Resource Utilization Innovation Team at Shaanxi University of Technology.

References

[1] S.A. Khan, I. Hussain, A.K. Thakur, et al., Energy Storage Mater. 65 (2024) 103144.
[2] D. Song, J. Yu, M. Wang, et al., Energy Storage Mater. 61 (2023) 102870.
[3] S. Yuan, X. Huang, T. Kong, et al., Acc. Chem. Res. 57 (2024) 1550–1563.
[4] H. Zhang, L. Qiao, H. Kühnle, et al., Energy Environ. Sci. 16 (2023) 11–52.
[5] M. Hina, S. Bashir, K. Kamran, et al., J. Energy Storage 85 (2024) 110961.
[6] N. Al-Zubaidi, R. Smith, M. Kasper, P. Kumar, et al., Batteries 8 (2022) 50.
[7] E. Blumbergs, V. Serga, E. Platacis, et al., Metals 11 (2021) 1714.
[8] A.K. Shukla, S. Venugopalan, B. Hariprakash, J. Power Sources 100 (2001) 125–148.
[9] W.H. Zhu, Y. Zhu, Z. Davis, B.J. Tatarchuk, Appl. Energy 106 (2013) 307–313.
[10] Y. Xu, F.M. Mulder, Int. J. Hydrogen Energy 46 (2021) 19542–19553.
[11] S. Mandal, S Thangarasu, P.T. Thong, et al., J. Power Sources 485 (2021) 229336.
[12] J. Huang, L. Yan, D. Bin, et al., J. Mater. Chem. A 8 (2020) 5959–5967.
[13] W. Zhou, D. Zhu, J. He, et al., Energy Environ. Sci. 13 (2020) 4157–4167.
[14] W. Cao, J. Zhang, H. Li, Energy Storage Mater. 26 (2020) 46–55.
[15] P.G. Bruce, B. Scrosati, J.M. Tarascon, Angew. Chem. Int. Ed. 47 (2008) 2930–2946.
[16] L. Ma, N. Li, C. Long, et al., Adv. Funct. Mater. 29 (2019) 1906142.
[17] H.S. Hirsh, Y. Li, D.H.S. Tan, et al., Adv. Energy Mater. 10 (2020) 2001274.
[18] H. Zhang, Y. Gao, X. Liu, et al., Adv. Energy Mater. 13 (2023) 2300149.
[19] J.Y. Hwang, S.T. Myung, Y.K. Sun, Chem. Soc. Rev. 46 (2017) 3529–3614.
[20] J. Xie, D. Lin, H. Lei, et al., Adv. Mater. 36 (2024) 2306508.
[21] A. Sharma, R. Sharma, R.C. Thakur, L. Singh, J. Energy Chem. 82 (2023) 592–626.
[22] A. Naveed, H. Ai, T. Li, et al., Adv. Funct. Mater. 34 (2024) 2400949.
[23] K. Zhang, L. Wang, C. Ma, et al., Small 20 (2024) 2309154.
[24] S. Liu, R. Zhang, J. Mao, et al., Appl. Phys. Rev. 10 (2023) 021304.
[25] R. Rao, L. Chen, J. Su, et al., Battery Energy 3 (2024) 20230036.
[26] S. Khalid, N. Pianta, P. Mustarelli, R. Ruffo, Batteries 9 (2023) 47.
[27] J. Chen, S. Lei, S. Zhang, et al., Adv. Funct. Mater. 33 (2023) 2215027.
[28] X. Cai, Z. Hu, W. Deng, et al., Batteries Supercaps 7 (2024) e202300619.
[29] M.Z. Iqbal, R. Zahid, M.W. Khan, et al., Int. J. Hydrogen Energy 48 (2023) 8045–8070.
[30] L. Cheng, Q. Zhu, J. Liang, et al., ACS Appl. Mater. Interfaces 13 (2021) 54096–54105.
[31] T. Peng, Y. Xing, L. Mu, et al., Chin. Chem. Lett. (2024), doi:10.1016/j.cclet.2024.110039.
[32] Y. Zhao, P. Zhang, J. Liang, et al., Energy Storage Mater. 47 (2022) 424–433.
[33] N. Liu, X. Wu, Y. Yin, et al., ACS Appl. Mater. Interfaces 12 (2020) 28199–28205.
[34] Z. Zhou, S. Liu, J. Wang, et al., Appl. Surf. Sci. 614 (2023) 156259.
[35] Y. Yang, T. Shao, Y. Zhang, et al., J. Power Sources 564 (2023) 232863.
[36] X. Gu, J. Wang, X. Zhao, et al., J. Energy Chem. 85 (2023) 30–38.
[37] J.J. Ye, P.H. Li, H.R. Zhang, et al., Adv. Funct. Mater. 33 (2023) 2305659.
[38] X. Cai, Y. Zhang, H. Cheng, et al., Small 19 (2023) 2304668.
[39] M. Liu, K. Zhu, K. Wan, et al., ACS Appl. Mater. Interfaces 15 (2023) 28073–28083.
[40] B. Dai, X. Shen, T. Chen, et al., Dalton Trans. 53 (2024) 8335–8346.
[41] R. Trócoli, G. Kasiri, F. La Mantia, J. Power Sources 400 (2018) 167–171.
[42] L. Zhang, L. Chen, X. Zhou, Z. Liu, Sci. Rep. 5 (2015) 18263.
[43] M. Tang, Q. Zhu, P. Hu, et al., Adv. Funct. Mater. 31 (2021) 2102011.
[44] J. Wang, Y. Yang, Y. Wang, et al., ACS Nano 16 (2022) 15770–15778.
[45] Y. Li, Y. Wang, Y. Xu, et al., Small 18 (2022) 2202214.
[46] M. Yang, H. Huang, S. Shen, et al., Chin. Chem. Lett. (2024), doi:10.1016/j.cclet.2024.109988.
[47] S.C.R. Niragatti, S.T.V. Madhukar, J. Kim, K. Yoo, J. Power Sources 587 (2023) 233716.
[48] L. Wang, J. Zheng, Mater. Today Adv. 7 (2020) 100078.
[49] J. Bai, S. Hu, L. Feng, et al., Chin. Chem. Lett. 35 (2024) 109326.
[50] Y. Liu, Y. Liu, X. Wu, Chin. Chem. Lett. 34 (2023) 107839.
[51] G. Li, L. Sun, S. Zhang, et al., Adv. Funct. Mater. 34 (2024) 2301291.
[52] S. Xie, X. Li, Y. Li, et al., Chem. Record 22 (2022) e202200201.
[53] P. He, S. Chen, Electrochem. Sci. Adv. 2 (2022) e2100090.
[54] H. Cao, Z. Zheng, P. Norby, et al., Small 17 (2021) 2100558.
[55] N. Zhang, Y.R. Ji, J.C. Wang, et al., J. Energy Chem. 82 (2023) 423–463.
[56] J. Liu, Z. Shen, C.Z. Lu, J. Mater. Chem. A 12 (2024) 2647–2672.
[57] J. Chen, W. Zhao, J. Jiang, et al., Energy Storage Mater. 59 (2023) 102767.
[58] F. Ma, Y. Wu, G. Wei, et al., J. Solid State Electrochem. 23 (2019) 2213–2224.
[59] L. Gan, F. Liu, X. Yuan, et al., Front. Energy 17 (2023) 775–781.
[60] N. Naresh, S. Eom, S. Hwan Jeong, et al., Appl. Surf. Sci. 606 (2022) 154932.
[61] D. Bin, Y. Wang, A.G. Tamirat, et al., ACS Sustain. Chem. Engin. 9 (2021) 3223–3231.
[62] S. Islam, S. Lee, S. Lee, et al., Chem. Engin. J. 446 (2022) 137069.

[63] Q. Liu, Z. Ma, Z. Chen, et al., Chem. Commun. 58 (2022) 8226–8229.
[64] Y. Li, X. Liu, T. Ji, et al., Chin. Chem. Lett. 36 (2025) 109551.
[65] P. He, G. Zhang, X. Liao, et al., Adv. Energy Mater. 8 (2018) 1702463.
[66] F. Wu, Y. Wang, P. Ruan, et al., Mater. Today Energy 21 (2021) 100842.
[67] G. Cui, Y. Zeng, J. Wu, et al., Adv. Sci. 9 (2022) 2106067.
[68] Y. Zhang, Y. Liu, Z. Liu, et al., J. Energy Chem. 64 (2022) 23–32.
[69] M. Zhou, Y. Chen, G. Fang, S. Liang, Energy Storage Mater. 45 (2022) 618–646.
[70] H. Liu, Q. Zhou, Q. Xia, et al., J. Energy Chem. 77 (2023) 642–659.
[71] S.J. Kim, C.R. Tang, G. Singh, et al., Chem. Mater. 32 (2020) 2053–2060.
[72] Y. Liu, J. Zhi, T.K.A. Hoang, et al., ACS Appl. Energy Mater. 5 (2022) 4840–4849.
[73] Y. Dai, C. Zhang, J. Li, et al., Adv. Mater. 36 (2024) 2310645.
[74] Y. Li, J. Wang, S. Wang, et al., Energy Storage Mater. 66 (2024) 103245.
[75] W. Wang, C. Yang, X. Chi, et al., Energy Storage Mater. 53 (2022) 774–782.
[76] N. Zhang, F. Cheng, J. Liu, et al., Nat. Commun. 8 (2017) 405.
[77] Y. Huang, Z. Li, S. Jin, et al., Carbon 167 (2020) 431–438.
[78] Y. Zong, H. He, Y. Wang, et al., Adv. Energy Mater. 13 (2023) 2300403.
[79] Y. Song, P. Ruan, C. Mao, et al., Nano-Micro Lett. 14 (2022) 218.
[80] Y. Zhang, X. Li, L. Fan, et al., Cell Rep. Phys. Sci. 3 (2022) 100824.